

Research Article

Tuning Optical Nonlinearity of Laser-Ablation-Synthesized Silicon Nanoparticles via Doping Concentration

Lianwei Chen,¹ Xiao-fang Jiang,² Ziming Guo,¹ Hai Zhu,² Tsung-Sheng Kao,³ Qing-hua Xu,² Ghim Wei Ho,¹ and Minghui Hong³

¹ Engineering Science Program, National University of Singapore, 4 Engineering Drive 3, Singapore 117576

² Department of Chemistry, National University of Singapore, 3 Science Drive 3, Singapore 117543

³ Department of Electrical and Computer Engineering, National University of Singapore, 4 Engineering Drive 3, Singapore 117576

Correspondence should be addressed to Minghui Hong; elehmfh@nus.edu.sg

Received 13 November 2013; Accepted 24 January 2014; Published 3 March 2014

Academic Editor: Mohsen Rahmani

Copyright © 2014 Lianwei Chen et al. This is an open access article distributed under the Creative Commons Attribution License, which permits unrestricted use, distribution, and reproduction in any medium, provided the original work is properly cited.

Silicon nanoparticles at different doping concentrations are investigated for tuning their optical nonlinear performance. The silicon nanoparticles are synthesized from doped silicon wafers by pulsed laser ablation. Their dispersions in water are studied for both nonlinear absorption and nonlinear refraction properties. It is found that the optical nonlinear performance can be modified by the doping concentration. Nanoparticles at a higher doping concentration exhibit better saturable absorption performance for femtosecond laser pulse, which is ascribed to the free carrier absorption mechanism.

1. Introduction

The optical nonlinear properties of nanomaterials have been extensively studied for the applications in high power laser devices. Among all these materials, silicon materials have triggered particularly high research interests because of their potential to be integrated with microelectronics [1, 2]. One of the primary arguments in favor of silicon optical materials is the possibility to build chip-scale photonic devices, which motivates intensive investigations on optical nonlinear properties of silicon materials in nanoscale [3–6].

In addition to its compatibility with the industry, silicon nanomaterials have many other advantages. Traditional materials like gold and silver are not cost efficient. Comparing to them, silicon has a rich source of supply and low processing cost. Different from most of organic optical nonlinear materials, silicon is promising for the biomedical applications due to its minimum toxicity. Synthesis methods have been reported to produce pure silicon materials with little chemical precursors [7, 8]. Meanwhile, the flourishing silicon industry and mature processing technique make it possible to precisely fabricate silicon nanoscale structures with modified intrinsic properties. Therefore, silicon emerges as a good candidate

to be a cheap and environmental friendly optical nonlinear material.

In the past decades, various silicon nanostructures were studied for their unique optical properties, such as porous silicon materials, silicon nanofibers, silicon nanoclusters, and nanoparticles [3, 9–14]. In these studies, silicon morphology was reported to be an important factor affecting the optical nonlinearity. Meanwhile, researchers also studied the silicon in different surrounding matrices, which was crucial for the optical nonlinear performance [14]. Other key factors include the density of free carriers. Since free carrier absorption is a nonlinear process, better optical nonlinearity is expected for silicon material with a large number of free carriers [12]. However, insufficient experiment data on the effect of the free carrier concentration have been reported. In this paper, a set of experiments are designed and presented to provide a better understanding on how the optical nonlinearity is affected by the density of free carriers.

The change of free carrier density is achieved by the tuning of the doping concentration in silicon. The dispersions of the silicon nanoparticles in water are synthesized and studied for the optical nonlinearity. These Si nanoparticles are produced by pulsed laser ablation in deionized (DI) water

TABLE 1: Surface resistivity and doping concentration of silicon wafers.

Number	Surface resistivity ($\Omega\cdot\text{cm}$)	Doping concentration (cm^{-3})
P1	0.01	$8.1E18$
P2	1.50	$1.0E16$
P3	4.90	$2.8E15$
P4	10.50	$1.3E15$
P5	16.50	$8.3E14$
N1	0.80	$8.4E16$
N2	0.10	$8.2E16$
N3	4.50	$1.0E15$
N4	8.00	$5.6E14$
N5	19.0	$2.3E14$

to form a stable dispersion. Nonlinear optical properties are characterized by the open and close aperture Z -scan methods. It is found that the increase of doping concentration enhances the optical nonlinear response, which opens a new way to tune the optical nonlinearity. Different from the modification of the morphology and environment, it is more flexible to tune the optical nonlinearity by simply varying the doping concentration.

2. Synthesis of Nanoparticle Dispersion

One-side polished silicon wafers were bought from the LiJingKeJi Ltd. N-type samples were doped with phosphorus and P-type samples were doped with boron. For each sample, the average sheet resistivity was recorded. The doping concentrations were calculated from the sheet resistance [15]. All these data are summarized in Table 1.

Pulsed laser ablation was applied to synthesize the silicon nanoparticles [16, 17]. In each experiment, a clean silicon wafer in the dimension of $1\text{ cm} \times 1\text{ cm}$ was positioned at the center of a 25 mL glass beaker, with the unpolished side facing towards the incident laser beam. The beaker was then put into a sample holder on the processing stage. The diagram of the experimental setup is shown in Figure 1(a), which was discussed in the previous work [18, 19]. The Nd:YAG fiber laser at the wavelength of 1064 nm (IDI Laser Service) was used for the laser ablation. The pulse duration (full width at half maximum) was 1.5 ns. The repetition rate was 60 kHz and the focal length used was 10 cm.

The laser beam was programmed to scan over a $1\text{ cm} \times 1\text{ cm}$ area for 900 times. A rectangular scanning pattern was chosen and the scanning speed was set at 1 mm/s. The laser fluence for the synthesis of silicon nanoparticles was kept at $0.8\text{ J}/\text{cm}^2$ at the focal point throughout the process. The entire process took about 6 minutes. After the laser ablation was completed, the color of the solvent changed into light brown, which resulted from the dispersion of the silicon nanoparticles inside the water.

Same parameters for the laser ablation were applied to synthesize silicon nanoparticles at different doping concentrations. The dispersions were collected and sonicated for 30

minutes to ensure the silicon nanoparticles are being well-dispersed in water. All the silicon nanoparticles' dispersions were placed at rest for one day to test the stability and no aggregations were observed. To calculate the nanoparticles' concentration, 30 cycles of the laser ablation were repeated on one silicon wafer and the average weight change per cycle was calculated. The mass loss of the silicon wafer in each cycle equals the total mass of the silicon nanoparticles synthesized and the nanoparticles' concentration can be estimated to be 5 mM.

3. Results and Discussion

3.1. Silicon Nanoparticles' Morphology and Size Distribution. SEM images were taken to characterize the morphology and size distribution of the silicon nanoparticles synthesized by the laser ablation. The dispersion was dropped onto an undoped silicon substrate and then observed under a high resolution Jeol JSM7001F SEM. The image of the silicon nanoparticles' morphology is shown in Figure 1(b). It is clear that most silicon nanoparticles are in sphere shape. The sizes of 100 nanoparticles were measured and the size distribution is shown in Figure 1(c). It can be seen that the size distribution ranges broadly from 0 to 400 nm, while the distribution peak locates at 100–200 nm. It is found in our experiment that, regardless of the doping concentration, the size distribution is similar to different samples. A schematic diagram of the laser ablation mechanism for the silicon nanoparticles' synthesis is shown in Figure 1(d). In the synthesis process, a rapid transfer of the energy from photons to the lattice causes the silicon materials to evaporate, which results in the generation of expanding plasma. This plasma is made of energetic species including atoms, molecules, ions, clusters, and dopants. During the expanding process, the plasma is confined by the surrounding water molecules under high pressure. The energetic species in the plasma collide with the surrounding water molecules and the kinetic energy is reduced. This strong hyperthermal reaction between the ablated energetic species and the surrounding water molecules promotes the nucleation and aggregation to form the nanoparticles. The silicon doping concentrations in our experiments are from 2.3×10^{14} to $8.1 \times 10^{18}\text{ cm}^{-3}$. The number of dopants is much smaller compared to that of silicon atoms. Therefore, the generation of energetic species is similar to silicon materials at different doping concentrations. In the same conditions, the plasma expansion and nucleation process are identical. As a result, silicon nanoparticles synthesized exhibit similar morphology and size distribution at different doping concentrations.

3.2. Absorption Spectrum of Silicon Nanoparticles. The absorption spectra of the silicon nanoparticles' dispersions were characterized by a Shimadzu UV-3600 UV-VIS-NIR spectrophotometer. The dispersions were heated on a hot plate to increase the nanoparticles' concentration in order to enhance the absorption features of silicon nanoparticles. The concentrated dispersions were sonicated for 10 minutes and transferred into a quartz cell with 1 cm light path length

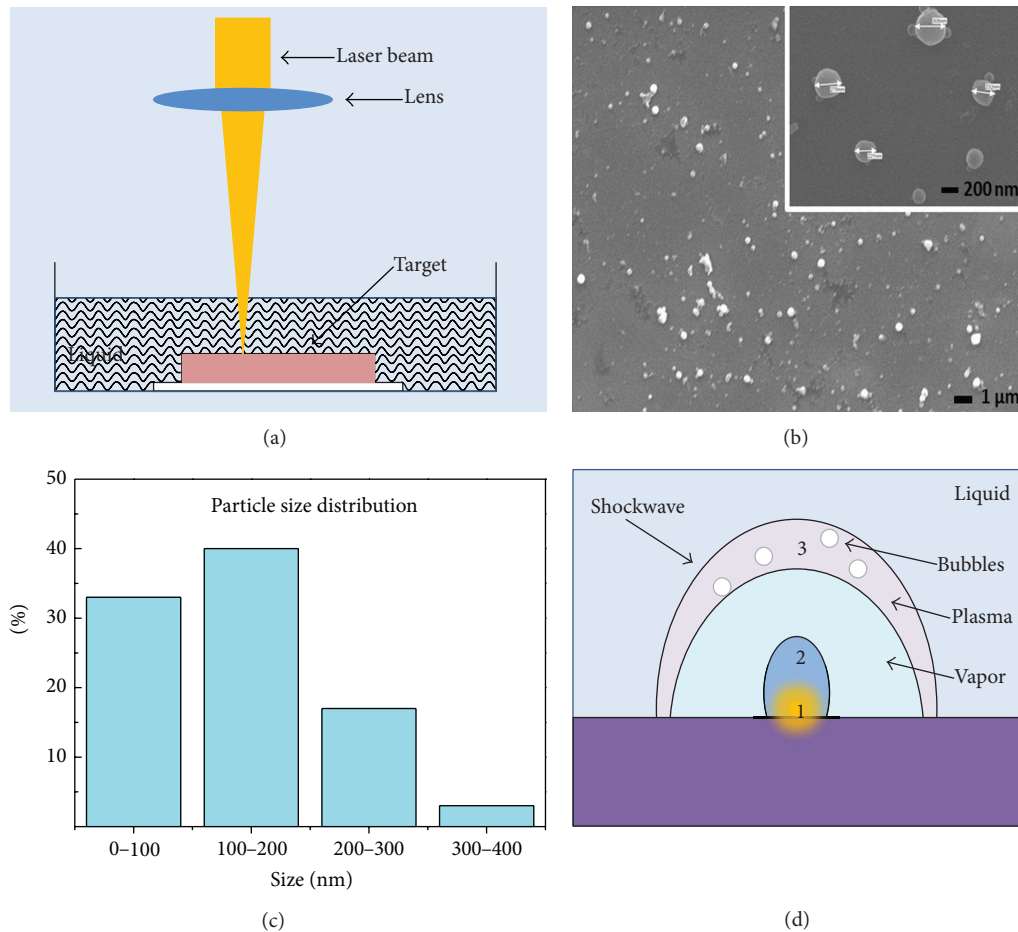


FIGURE 1: (a) Diagram of the laser ablation for silicon nanoparticles' synthesis. (b) SEM images of the silicon nanoparticles; inset: zoom-in image. (c) Particle size distribution of the silicon nanoparticles. (d) Laser plasma plume formation induced by laser ablation at different stages of (1) initial, (2) expansion, and (3) saturation.

for characterization. The absorption spectra from 350 to 1200 nm are shown in Figure 2. Inset of Figure 2 is the optical image of the silicon nanoparticles' dispersions to show their colors. The absorption spectra are similar to both P-type and N-type silicon nanoparticles' dispersions. The absorption increases at a short wavelength and reaches its peak at around 420 nm, which is in good agreement with the previous reported results [14, 20]. This absorption peak corresponds to the energy level of singularities in the electron density function [20].

3.3. Silicon Nanoparticles' Nonlinear Absorption and Nonlinear Refraction Properties. To characterize the nonlinear optical response, both open and close aperture Z-scan experiments were conducted. The Z-scan measurement was performed by using a regenerative Ti:Sapphire amplifier (Libra, Coherent), which gave output laser pulses with a central wavelength of 800 nm, pulse duration of around 100 fs, and repetition rate of 1 kHz. In our previous research, the same setup was applied to study the optical nonlinearity of graphene oxide [21].

The sample was sonicated for 30 minutes before the experiment to avoid aggregation. After sonication, the dispersion was transferred into a quartz cuvette with 1 mm optical path length, which was then placed at the starting location of the stage ($Z = -8$ mm). The Z-scan range was set from -8 to 8 mm. The aperture was adjusted to be fully open for the open aperture Z-scan measurement and 30% transmittance of the initial beam for the close aperture Z-scan experiment. Three cycles were repeated to reduce the experimental error and the average was calculated to plot the Z-scan curves.

The nonlinear absorption of the P-type silicon nanoparticles was examined by open aperture Z-scan method at the wavelength of 800 nm. The incident laser fluence is 40 mJ/cm^2 at the focal point. Results are shown in Figure 3(a). As a comparison, the transmittance curve of water was also plotted. It can be seen that the water does not show any change in the transmittance at different Z positions, which indicates that it does not have any observable nonlinear effect under our experiment conditions. Meanwhile, all the P-type silicon nanoparticles show clear features of the saturable absorption. Comparing the curves for samples at different doping concentrations, it can be found that the peak transmittance

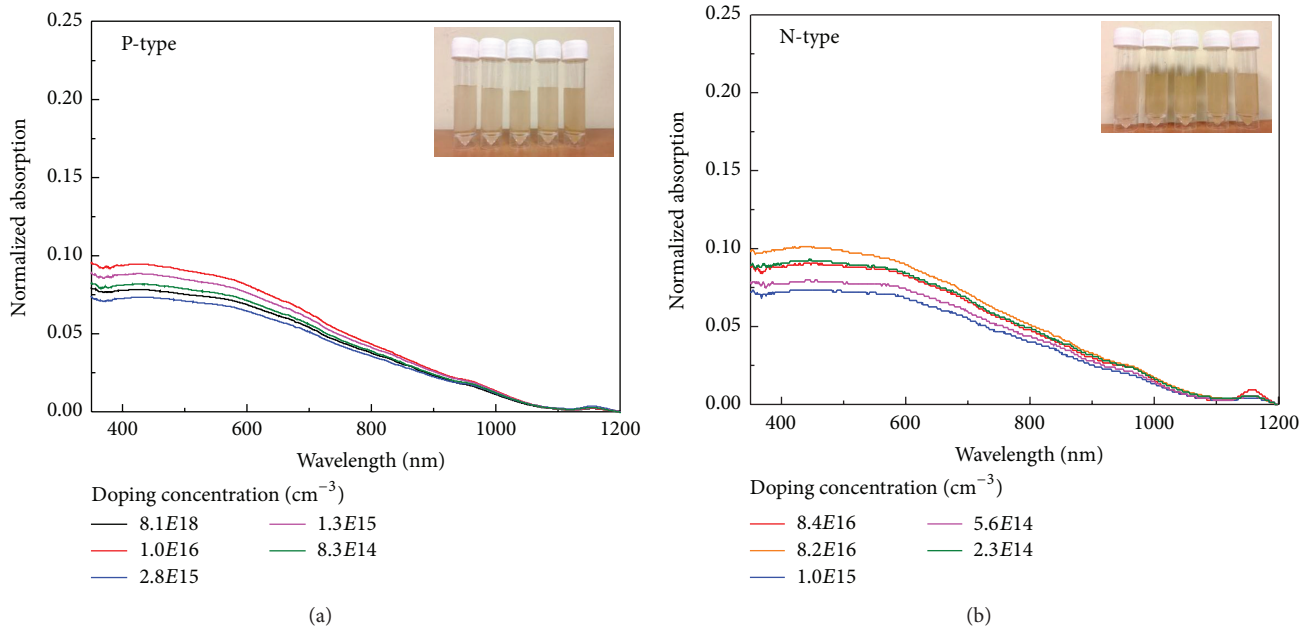


FIGURE 2: Absorption spectra for (a) P-type and (b) N-type silicon nanoparticles dispersions; inset: optical image of the dispersions.

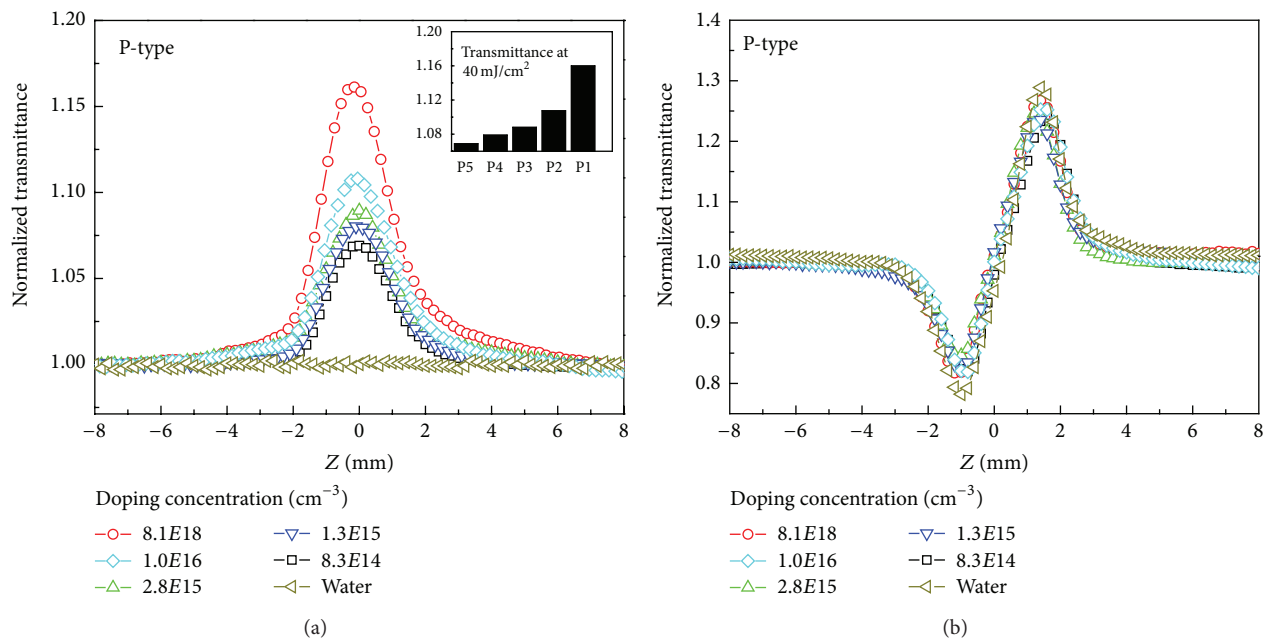


FIGURE 3: (a) Open aperture Z-scan curves for P-type silicon nanoparticle dispersions; inset: peak transmittance at different doping concentrations. (b) Close aperture Z-scan curves for P-type silicon nanoparticles' dispersions.

increases as the doping concentration increases, which indicates that the saturated nonlinear absorption is enhanced by the dopants. Among all the samples, the sample at the doping concentration of $8.1 \times 10^{18} \text{ cm}^{-3}$ presented a significant enhancement of the nonlinear absorption. Comparing to the silicon nanoparticles at the doping concentration of $8.3 \times 10^{14} \text{ cm}^{-3}$, the peak transmission was enhanced by 10%.

These different optical nonlinear responses related to the doping concentration can be explained by the mechanism of free carrier absorption [12]. Once generated, the free carriers can be promoted to a higher energy level by the absorption of photons. The probability for one free carrier to jump into a certain level is defined as the cross section. The saturated absorption is caused by the different cross

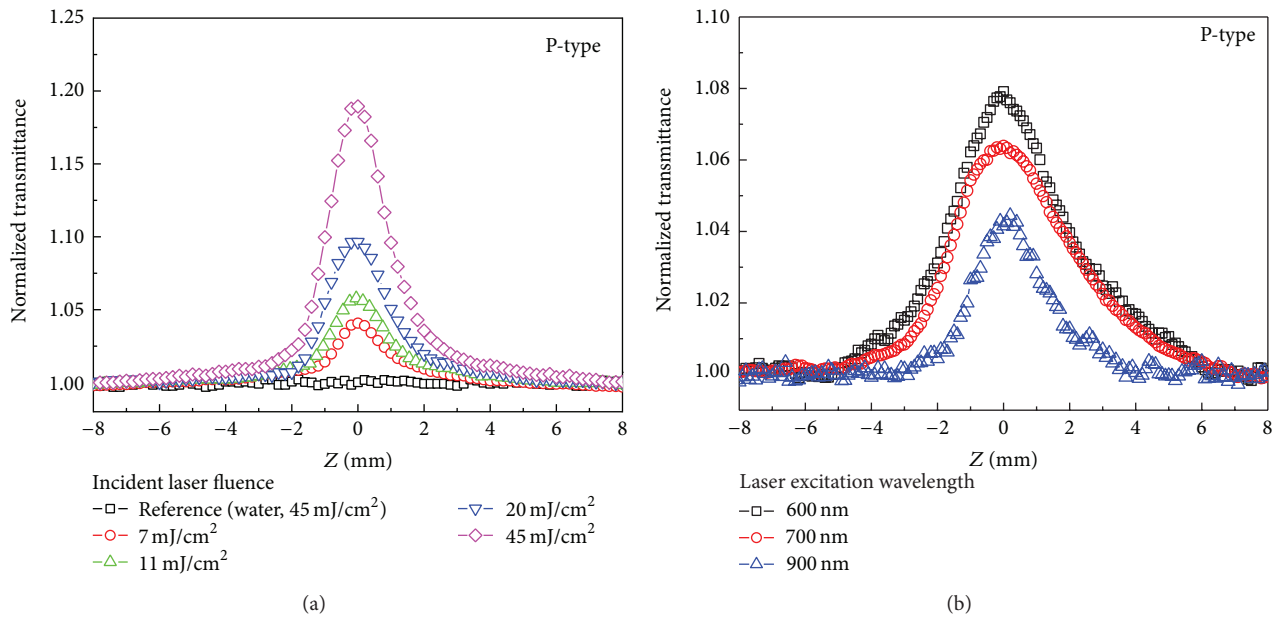


FIGURE 4: (a) Open aperture Z-scan curves at different incident laser fluences at the focal point. (b) Open aperture Z-scan curves at the laser excitation wavelengths of 600, 700, and 900 nm.

sections of the excitation levels. When the cross section for a higher excitation level is small, free carriers are not likely to jump up to the higher level and fail to absorb the laser energy, which causes the absorption to be “saturated” and the transmission to increase. The free carrier absorption is clearly an accumulative process, which relies on the buildup of the free carrier population. The nonlinear effect is in positive correlation with the density of the free carriers. When more free carriers fail to jump up to a higher level, the absorption becomes saturated more readily; thus, the increase of the free carriers can enhance the optical nonlinearity. A heavily doped sample has a larger number of free carriers, which is consistent with our observation that the sample with the highest doping concentration shows the most significant enhancement of the saturable absorption [12].

Close aperture Z-scan was conducted to verify whether the doping concentration influences the optical nonlinear refraction of the silicon nanoparticles. The transmittance curves are summarized in Figure 3(b). Experimental conditions were the same as those in the open aperture Z-scan measurement except that the aperture was set to 30% transmittance of the initial beam. The transmittance of water was also plotted as a reference, which exhibits the features of the self-focusing. The curves for the silicon nanoparticles’ dispersions and water are very similar. The reason can be explained as follows. The refractive index variation at different laser intensities is responsible for the nonlinear optical effect. Since the concentration of the silicon nanoparticles is low in water, refractive index variation is mainly affected by water. As a consequence, little enhancement of nonlinear refraction can be observed.

To build up a comprehensive understanding of the optical nonlinear response, the open aperture Z-scan measurements

with different excitation fluences and wavelengths were performed. The results on the P-type silicon nanoparticles with the doping concentration of $8.1 \times 10^{18} \text{ cm}^{-3}$ were chosen to be presented for illustration purpose. The results for laser fluence dependence at the excitation wavelength of 800 nm are shown in Figure 4(a). It is clear that the peak transmittance increases with the incident laser fluence. This observation can be ascribed to more free carriers generated at the higher laser fluence. Furthermore, comparing to other samples, a less intensive laser excitation is required to reach an identical peak transmittance. At the incident laser fluence of 11 mJ/cm^2 , the peak transmittance is 1.06 (Note: the transmittance is normalized to the linear transmittance at the initial Z-scan position, where there is no nonlinear absorption. 1.06 means the peak transmittance is 106% of the linear transmittance at the initial Z-scan position). For sample at the doping concentration of $8.3 \times 10^{14} \text{ cm}^{-3}$, the incident laser fluence needs to be increased to 40 mJ/cm^2 to have a comparable peak transmittance around 1.06, which is shown in Figure 3(a). As the identical peak transmittance means the same level of nonlinear absorption, it can be concluded that, in order to achieve an identical level of saturated nonlinear absorption, samples at high doping concentrations need a less intense laser than the samples at low doping concentrations. For the highly doped samples, its high free carrier density enables electrons to be more readily excited by laser pulses, which explains why they need lower laser fluence to achieve the same nonlinear response.

The broadband performance was also characterized at the laser excitation wavelength of 600, 700, and 900 nm using an optical parametric amplifier (Topas C). The incident laser fluence was set at 11 mJ/cm^2 at all these wavelengths.

The transmittance curves of the open aperture Z-scan measurement are shown in Figure 4(b). It can be seen that silicon nanoparticles exhibit optical nonlinear responses at all these excitation laser wavelengths and the optical nonlinear response is the strongest at the wavelength of 600 nm. This can be explained by the higher absorptions of silicon nanoparticles at a short wavelength, as shown in Figure 2. A larger absorption results in a larger amount of energy transferred to the silicon nanoparticles upon excitation. As a consequence, more free carriers are generated and excited. As these free carriers are hindered to jump up to a higher level due to the small cross section, the absorption becomes more saturated, which explains the enhancement of the optical nonlinearity.

The optical nonlinear response of N-type silicon samples was also characterized using the same Z-scan setups in our experiments. It was discovered that the increase of the doping concentration can enhance the nonlinear absorption, which can be explained similarly using the free carrier absorption mechanism. However, at same doping concentration, P-type silicon nanoparticles show stronger saturable absorption behavior than N-type silicon nanoparticles, which indicates that P-type silicon nanoparticles have better nonlinear response. This difference is due to their different cross sections of the excitation levels in two cases. The free carriers for P-type and N-type silicon materials are holes and electrons, respectively. Holes and electrons have different effective masses and momentum relaxing time, which influence the cross sections of the excitation levels [22].

4. Conclusions

Silicon nanoparticles' dispersions were synthesized by the pulsed laser ablation and their optical nonlinear responses were investigated. Under the same synthesis conditions, these silicon nanoparticles have similar morphology and size distribution. It is shown that the increase of the doping concentration leads to a stronger nonlinear absorption, while the nonlinear refraction is not changed much. This enhancement can be explained by the free carrier absorption mechanism. The characterization at different wavelengths proves that the silicon nanoparticles have a broadband nonlinear response and the optical nonlinearity is stronger at a shorter wavelength. This research reveals the possibility to tune the optical nonlinearity of silicon nanoparticles via doping concentration.

Conflict of Interests

The authors declare that there is no conflict of interests regarding the publication of this paper.

Acknowledgment

The authors are grateful for financial support from the Temasek Defence Systems Institute (TDSI) under Project no. TDSI/11-013/1A.

References

- [1] B. Jalali and S. Fathpour, "Silicon photonics," *Journal of Lightwave Technology*, vol. 24, no. 12, pp. 4600–4615, 2006.
- [2] M. Lipson, "Guiding, modulating, and emitting light on Silicon—challenges and opportunities," *Journal of Lightwave Technology*, vol. 23, no. 12, pp. 4222–4238, 2005.
- [3] R. Dekker, N. Usechak, M. Först, and A. Driessen, "Ultrafast nonlinear all-optical processes in silicon-on-insulator waveguides," *Journal of Physics D*, vol. 40, no. 14, pp. R249–R271, 2007.
- [4] L. A. Golovan and V. Y. Timoshenko, "Nonlinear-optical properties of porous silicon nano-structures," *Journal of Nanoelectronics and Optoelectronics*, vol. 8, pp. 223–239, 2013.
- [5] J. Leuthold, C. Koos, and W. Freude, "Nonlinear silicon photonics," *Nature Photonics*, vol. 4, no. 8, pp. 535–544, 2010.
- [6] Q. Lin, O. J. Painter, and G. P. Agrawal, "Nonlinear optical phenomena in silicon waveguides: modeling and applications," *Optics Express*, vol. 15, no. 25, pp. 16604–16644, 2007.
- [7] R. Intartaglia, K. Bagga, M. Scotto, A. Diaspro, and F. Brandi, "Luminescent silicon nano-particles prepared by ultra short pulsed laser ablation in liquid for imaging applications," *Optical Materials Express*, vol. 2, pp. 510–518, 2012.
- [8] N. G. Semaltianos, S. Logothetidis, W. Perrie et al., "Silicon nanoparticles generated by femtosecond laser ablation in a liquid environment," *Journal of Nanoparticle Research*, vol. 12, pp. 573–580, 2010.
- [9] P. Cheng, H. Zhu, Y. Bai, Y. Zhang, T. He, and Y. Mo, "Third-order nonlinear optical response of silicon nanostructures dispersed in organic solvent under 1064 nm and 532 nm laser excitations," *Optics Communications*, vol. 270, no. 2, pp. 391–395, 2007.
- [10] V. Klimov, D. McBranch, and V. Karavanskii, "Strong optical nonlinearities in porous silicon: femtosecond nonlinear transmission study," *Physical Review B*, vol. 52, no. 24, pp. R16989–R16992, 1995.
- [11] S. B. Korovin, V. I. Pustovoi, and A. N. Orlov, "High nonlinear susceptibility of the silicon based nanostructures," in *Proceedings of the International Conference on Advanced Laser Technologies (ALT '99)*, V. I. Pustovoy and V. I. Konov, Eds., pp. 472–478, 2000.
- [12] L. W. Tutt and T. F. Boggess, "A review of optical limiting mechanisms and devices using organics, fullerenes, semiconductors and other materials," *Progress in Quantum Electronics*, vol. 17, no. 4, pp. 299–338, 1993.
- [13] S. Vijayalakshmi, F. Shen, and H. Grebel, "Artificial dielectrics: nonlinear optical properties of silicon nanoclusters at $\lambda = 532$ nm," *Applied Physics Letters*, vol. 71, no. 23, pp. 3332–3334, 1997.
- [14] E. Koudoumas, O. Kokkinaki, M. Konstantaki et al., "Nonlinear optical response of silicon nanocrystals," *Optical Materials*, vol. 30, no. 2, pp. 260–263, 2007.
- [15] G. Masetti, M. Severi, and S. Solmi, "Modeling of carrier mobility against carrier concentration in arsenic-, phosphorus-, and boron-doped silicon," *IEEE Transactions on Electron Devices*, vol. 30, no. 7, pp. 764–769, 1983.
- [16] T. C. Chong, M. H. Hong, and L. P. Shi, "Laser precision engineering: from microfabrication to nanoprocessing," *Laser and Photonics Reviews*, vol. 4, no. 1, pp. 123–143, 2010.
- [17] M. H. Hong, "Laser-material interaction and its applications in surface micro/nano-processing," in *Proceedings of the International Symposium on High Power Laser Ablation*, C. R. Phipps,

- Ed., pp. 293–302, American Institute of Physics, Melville, NY, USA, 2010.
- [18] G. X. Chen, M. H. Hong, T. C. Chong, H. I. Elim, G. H. Ma, and W. Ji, “Preparation of carbon nanoparticles with strong optical limiting properties by laser ablation in water,” *Journal of Applied Physics*, vol. 95, no. 3, pp. 1455–1459, 2004.
- [19] G. X. Chen, M. H. Hong, T. S. Ong et al., “Carbon nanoparticles based nonlinear optical liquid,” *Carbon*, vol. 42, no. 12-13, pp. 2735–2737, 2004.
- [20] S. B. Korovin, A. N. Orlov, A. M. Prokhorov et al., “Nonlinear absorption in silicon nanocrystals,” *Quantum Electronics*, vol. 31, no. 9, pp. 817–820, 2001.
- [21] X.-F. Jiang, L. Polavarapu, S. T. Neo, T. Venkatesan, and Q.-H. Xu, “Graphene oxides as tunable broadband nonlinear optical materials for femtosecond laser pulses,” *Journal of Physical Chemistry Letters*, vol. 3, no. 6, pp. 785–790, 2012.
- [22] C. M. Wolfe, N. Holonyak, and G. E. Stillman, *Physical Properties of Semiconductors*, Prentice Hall, Upper Saddle River, NJ, USA, 1989.



Hindawi

Submit your manuscripts at
<http://www.hindawi.com>

